Sophocarpine inhibits TRP channels to produce anti-pruritic and analgesic effects in a mouse model of inflammatory itch and pain

Hekun Zeng[1], Peiyang Li[1], Dan Zhou[1], Zhe Zhang[1], Alexei Verkhratsky[2,3,4], Hong Nie[1*]

[1]International Cooperative Laboratory of Traditional Chinese Medicine Modernization and Innovative Drug Development of Chinese Ministry of Education (MOE), Guangdong Province Key Laboratory of Pharmacodynamic Constituents of TCM and New Drugs Research, College of Pharmacy, Jinan University, 601 Huangpu Avenue West, Guangzhou, 510632, China;

[2]Faculty of Biology, Medicine and Health, the University of Manchester, Manchester, United Kingdom;

[3]Achucarro Centre for Neuroscience, IKERBASQUE, Basque Foundation for Science, Bilbao, Spain;

[4]Department of Stem Cell Biology, State Research Institute Centre for Innovative Medicine, LT-01102, Vilnius, Lithuania.

[*]Corresponding authors：

Prof. Hong Nie

Tel: 86-20-85222810

Fax: 86-20-85224476

E-mail: hongnie1970@163.com

Running title: Sophocarpine relieves inflammatory itch and pain

Abstract

Background and objective: Itch, an unpleasant sensation prompting the urge to scratch, and pain, aimed at detecting potential harm through acute withdrawal or protective behaviors, are increasingly recognized as interconnected phenomena. The co-occurrence of itch and pain symptoms in various diseases impairs therapeutic efficacy and the quality of life. In this study, we investigated the potential antipruritic and analgesic effects of sophocarpine (SC), an active compound of *Sophorae Flavesentis Radix*, in a murine model of inflammatory itch and pain, and sought to elucidate the underlying mechanisms.

Method: The anti-pruritic and analgesic effects of three doses of SC (60 mg/kg, 30 mg/kg, 10 mg/kg) were tested by analyzing the scratching and wiping behaviors in squaric acid dibutylester (SABDE)-induced allergic contact dermatitis (ACD) mouse model accompany by itch and pain, respectively. Psoriasis area and severity index (PASI) score was used to test the anti-inflammatory effect of SC. The underlying mechanisms were studied by real-time quantitative polymerase chain reaction (RT-qPCR) and western blotting. Additionally, the anti-pruritic and analgesic effects of SC were further tested in mice with intradermal injection of allyl-isothiocyanate (AITC), a TRPA1 agonist, or capsaicin (CAP), a TRPV1 agonist, respectively. The relationships between SC, AITC, CAP and TRPV1, TRPA1 were simulated by

molecular docking.

Results: SC treatment significantly decreased scratching bouts and wipes, as well as the PASI score. Administration of SC reduced the mRNA and protein expression of both TRPA1 and TRPV1. Moreover, pretreatment of SC decreased scratching bouts and wipes induced by AITC as well as by CAP. Molecular docking revealed potential competitive binding between SC and AITC on TRPA1, and SC and CAP on TRPV1.

Conclusion: We demonstrated that SC has strong anti-pruritic and analgesic effects by targeting the TRPA1 and TRPV1 ion channels, and is a potential competitive inhibitor of TRPA1 and TRPV1. These findings suggest that SC has significant therapeutic potential in the therapy of diseases with inflammatory itch and pain.

Keywords: sophocarpine, anti-pruritic, analgesic, TRPA1, TRPV1.

1. Introduction

Itch is an unpleasant sensation that causes the need to scratch the affected area to remove puritogens thus causing temporary relief (1). Differing from the itch, pain-related harm detection instigates acute withdrawal or other protective behaviors. Itch and pain are distinct sensations both relying on interacting sensory subdivisions; however, opioids could inhibit pain but generate itch indicating distinct mechanisms for itch and pain (2).

Chronic itch and pain have broadly overlapping mediators and functions (3). For example, nerve growth factor could induce sensitization of primary afferents in both chronic itch and pain (4). Finding effective medicine targeting the common

67 mechanism to relieve itch and pain is required to avoid physical or mental issues
68 brought by both uncomfortable sensations coexisting.

69 In humans, the transient receptor potential (TRP) channel family covers 27
70 members classified into six groups of TRPC (canonical), TRPV (vanilloid), TRPM
71 (melastatin), TRPP (polycystin), TRPML (mucolipin), and TRPA (ankyrin); an
72 additional group of TRPN (NOMPC-like) is present in invertebrates and fishes. The
73 TRP channels are widely expressed through the nervous system and contribute in
74 particular to all types of sensing including thermal sensation, nociception,
75 chemisorption, equilibrioception and taste (5). The TRP channels are archetypal
76 cationic channels, many of which are highly permeable to Ca^{2+} ions (6). The TRPA1
77 and TRPV1 subfamilies contribute to both inflammatory itch and pain sensation (7).
78 Many pro-inflammatory mediators such as bradykinin, leukotrienes, tumour necrosis
79 factor-α (TNF-α), and interleukin-1β (IL-1β) can activate the TRPA1 and TRPV1
80 channels to mediate pain (8). In addition, TRPA1 was suggested to mediate
81 histamine-independent itch, whereas TRPV1 mediate histamine-dependent itch (9,
82 10).

83 *Sophorae Flavesentis Radix* (SFR), a Traditional Chinese Medicine, has been
84 used to relieve itch and pain in clinics in China for thousands of years. In our previous
85 study, we identified, by cell membrane chromatography, sophocarpine (SC) as a
86 bioactive compound that could bind to receptors on the plasma membrane of cells in
87 dorsal root ganglion (DRG) (11). In the present study, we employed an allergic
88 contact dermatitis (ACD) mouse model of itch and pain to investigate the analgesic

89 and anti-pruritic effect of SC and underlying pathways, and test its effect on the
90 TRPA1 and TRPV1, mediating itch and pain.

91 2. Materials and Methods

92 2.1 Animal

93 Male mice (6-week-old, 20±2 g) were purchased from the SPF (Beijing)
94 Biotechnology Co. Ltd. (Certificate NO. SCXK (Beijing) 2016-0002). All mice were
95 housed under a cycle of 12 h light/dark and given standard laboratory food and tap
96 water in the Jinan University Medical School's Laboratory Animal Management
97 Center (Certificate No. SYXK (Guangdong) 2017-0174). All experimental procedures
98 and animal welfare strictly followed the Guide for the Care and Use of Laboratory
99 Animals and related to Jinan University's ethical regulations (Approval No:
100 IACUC-20180621-07).

101 2.2 Establishment of allergic contact dermatitis mouse model

102 The ACD, or Contact Hypersensitivity (CHS) mouse model was established as
103 described by applying squaric acid dibutylester (SADBE, Tokyo Chemical Inc.,
104 Tokyo, Japan) dissolved in acetone (Guangzhou Chemical Reagent Factory,
105 Guangzhou, China) on the right cheek (12) (Figure 1). Briefly, the mice's abdomen
106 (1.5×1.5 cm^2) was shaved on Day -1. Starting from Day 1, 25 μL 1% SADBE (v/v)
107 was applied to the abdominal shaved area for three consecutive days once daily. The
108 mice's right cheek (0.8×0.8 cm^2) was shaved on Day 6, and 25 μL 1% SADBE was
109 applied to the cheek shaved area once daily for three consecutive days starting from

110 Day 8 to excite the ACD. The control group was treated with 25 μL pure acetone
111 instead of 1% SADBE.

112 **2.3 Drug administration and evaluation of spontaneous scratching and wiping**
113 **behaviors**

114 Three doses of SC (60, 30 and 10 mg/kg, Chengdu Push Bio-technology Co., Ltd,
115 Chengdu, China), capsazepine (CPZ, 30 mg/kg, Selleck Chemicals LLC, Houston,
116 TX, USA), dexamethasone (DEM, 5 mg/kg, Shanghai Macklin Biochemical Co., Ltd.,
117 Shanghai, China) and saline were administrated intragastrically (i.g.) through the
118 catheter on Day 11 (24 h after the third application of 1% SADBE on the cheek) as
119 shown in figure 1. To evaluate the spontaneous scratching bout and wiping behavior,
120 mice were placed in a separate, clear plastic container in 9×9×13 cm^3 with a small
121 amount of bedding inside, and a camcorder was positioned above the container to
122 record two mice at a time for 2 h, at 1 h after drug administration. Four mirrors were
123 placed with their bottoms aligned to the 4 lines of the square bottom of each container,
124 to give views of the mice from all 4 sides. Mice were trained for 2 hours daily from
125 Day 1 to Day 10 and were placed into the container 30 min before video recording to
126 let the mice get used to the surroundings. For each 2-hour video, the itch-like
127 scratching with the hindlimb and pain-like wiping with the forelimb was counted by
128 an investigator who was blinded to the experimental design (13, 14).

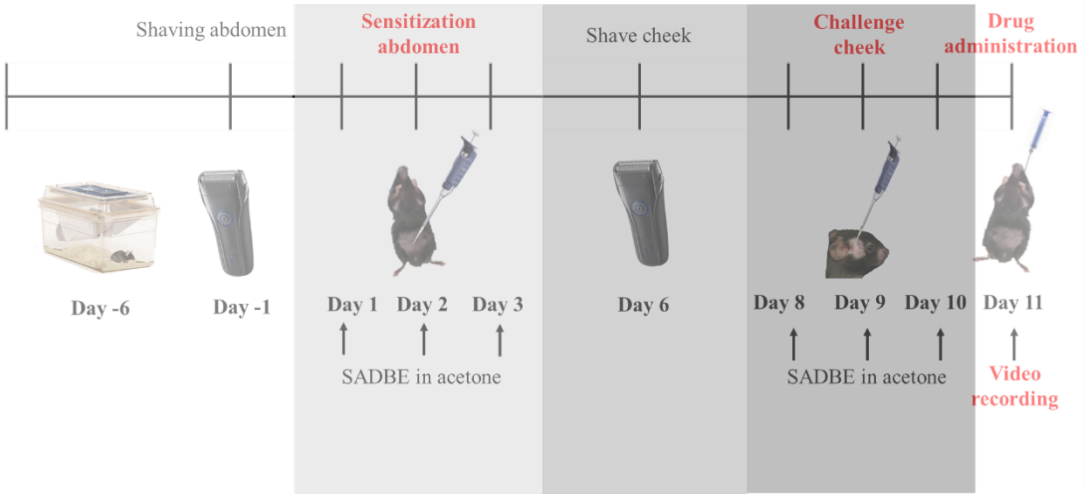

Figure 1. Experimental protocol for the establishment of ACD model on the cheek and drug intragastric administration. 70 C57BL/6 mice were randomly allocated into 7 groups: control group, ACD group, DEM group (5 mg/kg), CPZ group (30 mg/kg), and three doses of SC groups (60 mg/kg, 30 mg/kg, 10 mg/kg). Mice were trained daily from Day 1 to Day 10. On Day -1, the abdomen of the mice was shaved. From Day 1 to Day 3, 25 μL 1% SABDE was applied once daily onto the abdomens, except for the control group of mice who were applied with the same volume of acetone instead. On Day 6, the cheek of the mice was shaved. From Day 8 to Day 10, 25 μL 1% SABDE was applied onto the cheek once daily, except for the control group of mice who were applied with the same volume of acetone instead. On Day 11, mice in the control group and the ACD group were administrated i.g. with saline, the CPZ group with 30 mg/kg CPZ, and the SC groups with corresponding doses of SC. The behaviors were recorded for 2 h.

2.4 Measurement of skin-fold thickness and PASI score

The image of each mice's cheek skin was taken under brief anesthesia after the video recording in a standardized setup. The severity of the inflammation was rated

146 for the amount of erythema, thickening and scaling, each assessed independently on
147 the following scale: 0, none; 1, slight; 2, moderate; 3, marked; and 4, very marked.
148 The PASI score was calculated as the sum of the erythema, scaling and thickening
149 scores. The cheek fold thickness of each mouse was measured 3 times using a
150 micrometre (Mitutoyo, Tokyo, Japan), and the mean was calculated.

151 **2.5 Real-time quantitative polymerase chain reaction (RT-qPCR)**

152 After the measure of cheek fold thickness, mice were sacrificed and the
153 trigeminal ganglion (TG) from the treated side was immediately isolated. The mRNA
154 was extracted using TRIzol reagents (ThermoFisher Scientific, Waltham, MA, USA)
155 cDNA was synthesized from 100 μg of total RNA by Prime Script™ RT reagent kit
156 with gDNA Eraser (Takara, Tokyo, Japan). Each cDNA sample was amplified for the
157 gene of interest and β-actin in a 15 μL reaction volume TB Green™ Premix Ex Taq™
158 II (Takara, Tokyo, Japan). The PCR conditions were 95 °C for 30 s followed by 40
159 cycles of 95 °C for 5 s and 60 °C for 60 s. The whole procedure was performed
160 according to the manufacturer's instructions. The mRNA levels of all genes were
161 normalized to the measured mRNA values of the housekeeping gene β-actin. The
162 primers used are listed in Table 1.

163 Table 1 Primer sequences

Genes	Primer sequences
TRPV1-Forward	5′-ATCTTCACCACGGCTGCTTACT-3′
TRPV1-Reverse	5′-CACAAACAAACTCTTGAGGGATG-3′
TRPA1-Forward	5′-AATCTCTGTCCTCTGCATCACG-3′
TRPA1-Reverse	5′-ACAATGCAGTGGGGTATTTCC-3′
β-actin-Forward	5′-AGATGTGGATCAGCAAGCAGG-3′

β-actin-Reverse	5′-GCTCAGTAACAGTCCGCCTAGA-3′

164 **2.6 Western blotting**

165 After the measure of cheek fold thickness, mice were sacrificed, and the cheek
166 skin and TG from the treated side were immediately isolated. The total protein was
167 extracted using Cell lysis buffer for Western and IP (Beyotime Biotechnology,
168 Shanghai, China). 30 μg of each sample was added into 15% SDS gel. Protein
169 separation was performed at room temperature with a voltage of 90 V for 30 min
170 followed by 120V for 45-60 min, and protein transferring to the PVDF membrane was
171 performed on ice with a current of 250 mA for 1.5 h. Afterwards, the PVDF
172 membrane was washed 6 times with TBST on a shaking table at room temperature for
173 5 min each. Blocking was performed at room temperature using 5% skim milk
174 powder in TBST on a shaking table for 1 h. Afterwards, the PVDF membrane was
175 washed again 6 times with TBST on the shaking table at room temperature for 5 min
176 each. The primary antibodies (rabbit polyclonal anti-TRPV1 1:1000 (NBP1-97417,
177 Novus Biologicals, Littleton, CO, USA), rabbit polyclonal anti-TRPA1 1:2000
178 (NB100-98841, Novus Biologicals, Littleton, CO, USA) and mouse monoclonal
179 β-actin 1:1000 (8H10D10, CST, Danvers, MA)) were incubated with PVDF
180 respectively overnight at 4 ℃. After 6 times washing with TBST for 5 min each,
181 HRP-conjugated secondary antibodies (included goat anti-rabbit 1:5000 (A0208,
182 Beyotime Biotechnology, Shanghai, China) and goat anti-mouse 1:2000 (A0216,
183 Beyotime Biotechnology, Shanghai, China) was incubated with PVDF membrane on
184 the shaking table at room temperature for 2 h. After incubation, the PVDF membrane

185 was washed with TBST 6 times, 5 min each. The detection was performed with the
186 Super ECL detection reagent (Applygen, Beijing, China).

187 **2.7 CAP and AITC-induced behavioral testing**

188 50 C57BL/6 mice were randomly allocated into 5 groups: Control group, AITC
189 group, AITC+SC group, CAP group and CAP+SC group, in CAP and AITC-induced
190 behavior testing. The 10 mg/kg SC or the same volume of saline was administrated i.g.
191 for the CAP+SC and AITC+SC group or other groups at 1 h before CAP and AITC,
192 respectively. After adaptation for 30 min, 1 mg/kg CAP (Jiuding Chemical, Shanghai,
193 China, dissolved in 7% Tween-80), 1% AITC (w/v, Chengdu Herbpurify Co., Ltd,
194 Chengdu, China, dissolved in 7% Tween-80) and 10 μL 7% Tween-80 as the vehicle
195 was intradermally administrated into mice cheek of CAP groups, AITC groups and
196 control group respectively. In this assay, the video was recorded for 30 min following
197 CAP and AITC injection. The pain-like behavior and itch-like behavior were
198 measured as described in 2.3.

199 **2.8 Molecular Docking**

200 The AutoDock Vina in Chimera and ChimeraX were used for molecular docking
201 simulations and visualization of SC, CAP and AITC into active binding sites of
202 TRPA1 and TRPV1. The molecular structure of SC (ZINC3881784), CAP
203 (ZINC1530575) and AITC (ZINC1687017) was adopted from ZINC
204 (https://zinc.docking.org/).(15) The protein structure of TRPV1 (PDB ID: 3J5P) and
205 TRPA1 (PDB ID: 3J9P) was adopted from RCSB Protein Data Bank
206 (https://www.rcsb.org/).(16) Autodock Vina 1.1.2 in UCSF Chimera 1.17.3 was used

207 for molecules and proteins preprocessing, docking box determination and docking
208 simulations, according to a similar tutorial on https://vina.scripps.edu/. (17, 18) The
209 docking results were visualized and atomic distances of hydrogen bonds were
210 measured by ChimeraX 1.6.1. (19)

211 **2.9 Statistical analysis**

212 All the data was shown as mean±S.E.M. All statistical analyses were performed
213 using GraphPad Prism 9 (GraphPad Software, La Jolla, CA, USA). The comparisons
214 of quantitative data among groups were performed using one-way ANOVA, followed
215 by Bonferroni corrections for testing between individual means. A value of $p < 0.05$
216 was considered statistically significant. All figures were processed in GraphPad Prism
217 9.

218 # 3 Results

219 **3.1 SC reduced scratching and wiping behaviors in SADBE-induced ACD mice**

220 Mice in the ACD group exhibited a significantly greater number of scratching
221 bouts and wipes than in the control group (Figure 2). Compared with the ACD group,
222 mice in the DEM group, CPZ group, and all SC groups exhibited fewer scratching
223 bouts, while only SC groups exhibited fewer wipes (Figure 2). SC reduced mice
224 wiping behavior in a dose-dependent manner, whereas 60 mg/kg and 30 mg/kg SC
225 showed the same potency against scratching behavior, having however stronger effect
226 than 10 mg/kg dose (Figure 2).

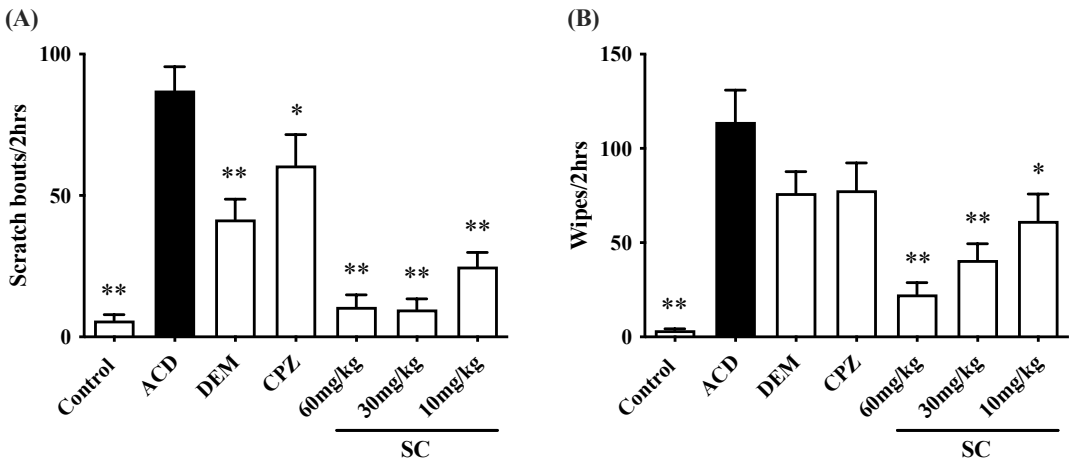

Figure 2. Effect of SC on relieving wiping and scratching on ACD mouse model. The mean of wipes (A) and the mean of scratching bouts (B) were evaluated for 2 h starting at 1 h after saline (control and ACD group), 5 mg/kg DEM (DEM group), 30 mg/kg CPZ (CPZ group), 60 mg/kg SC (60 mg/kg SC group), 30 mg/kg SC (30 mg/kg SC group), 10 mg/kg SC (10 mg/kg SC group) administration on ACD mice. $^{*}p < 0.05$, $^{**}p < 0.01$, compared with ACD group, error bars: S.E.M. n =10 mice /group.

3.2 SC improved the cheek skin inflammation in ACD mice

In the control group, we found no visual indications of redness, scaling or swelling of the cheek skin (Figure 3B). The ACD group demonstrated noticeable scaling, swelling and redness (Figure 3B). The skinfold thickness of the DEM group, 30 mg/kg SC group and 10 mg/kg SC group was lower than that of the ACD group, while there was no difference between the CPZ group, 60 mg/kg SC group and the ACD group (Figure 3A). Further analysis showed that the DEM group and SC groups had significantly lower PASI scores compared to the ACD group (Figure 3F). In the detailed scoring of the PASI scale, there was no difference between the DEM group,

all SC groups and the ACD group in erythema scoring; the DEM group and 60 mg/kg SC group scored lower in scaling score; and all groups scored lower in thickening score compared with those of the ACD group (Figure 3C, 3D, 3E).

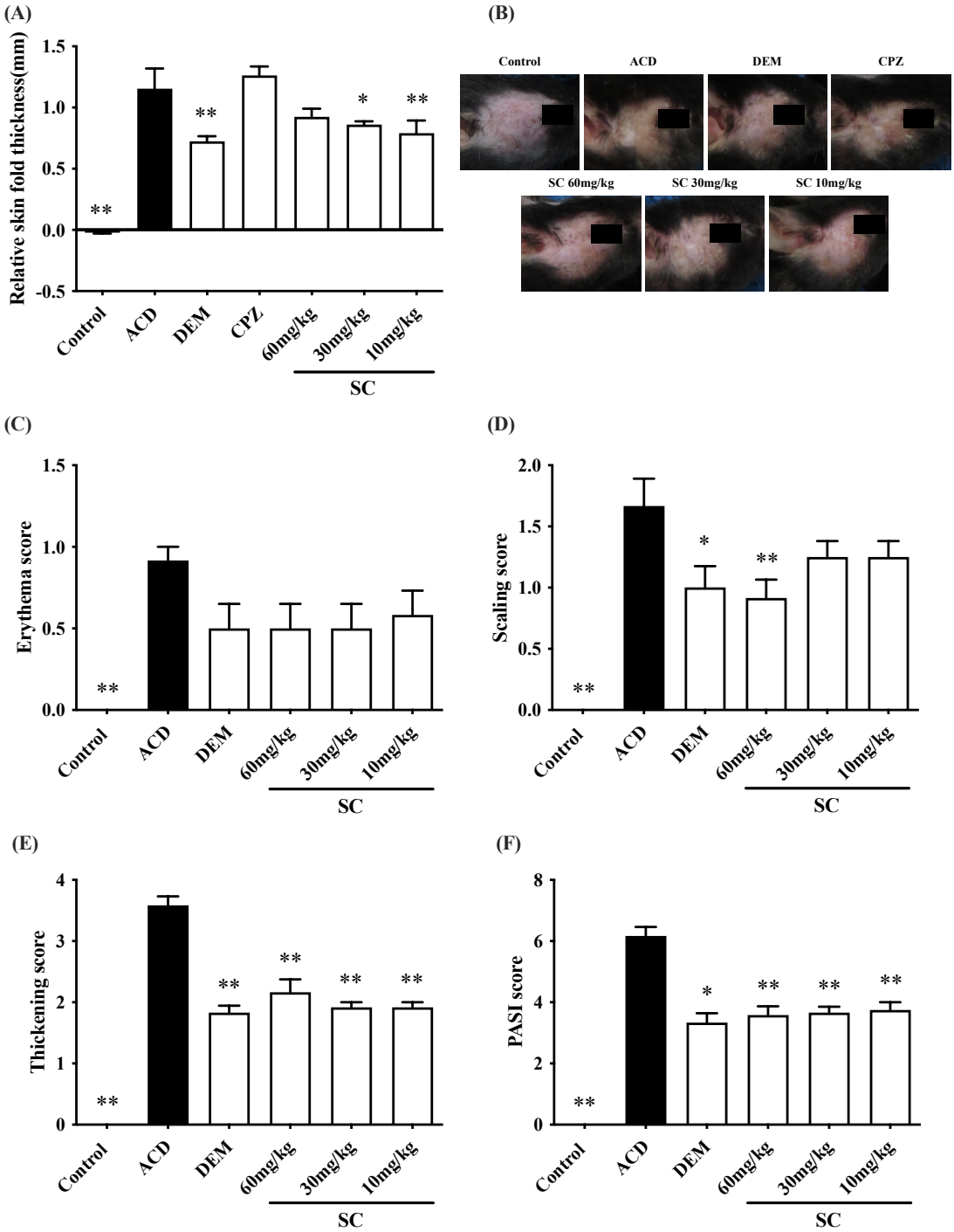

Figure 3. Effects of SC on thickness and severity of inflammation of the skin on ACD mouse model. The mean skin fold thickness (A) was measured after recording. (B)

Exemplary photographs of the mouse cheek skin in each experimental group show the visible change in the different treatment groups. The erythema (C), scaling (D), and thickening (E) were separately scored on a scale from 0 (none) to 4 (very marked). The PASI score (F) was taken as the sum of the erythema, scaling and thickening scores. $^{*}p < 0.05$, $^{**}p < 0.01$ for significance compared with the ACD group, error bars: S.E.M. n=10 mice/group.

3.3 SC reduced inflammation by downregulating the expression of the TNF-α and IL-1β in the skin

Expression of TNF-α and IL-1β mRNA in mice cheek skin was significantly greater in the ACD group, compared with that of the control group (Figure 4A, 4B). Compared with the ACD group, DEM and SC significantly downregulated expression of TNF-α and IL-1β mRNA (Figure 4A, 4B). Western blotting revealed a significantly higher TNF-α and TRPV1 protein expression in the ACD group compared with the control group (Figure 4C, 4D). Compared with the ACD group, DEM and SC decreased TNF-α and IL-1β protein expression (Figure 4C, 4D).

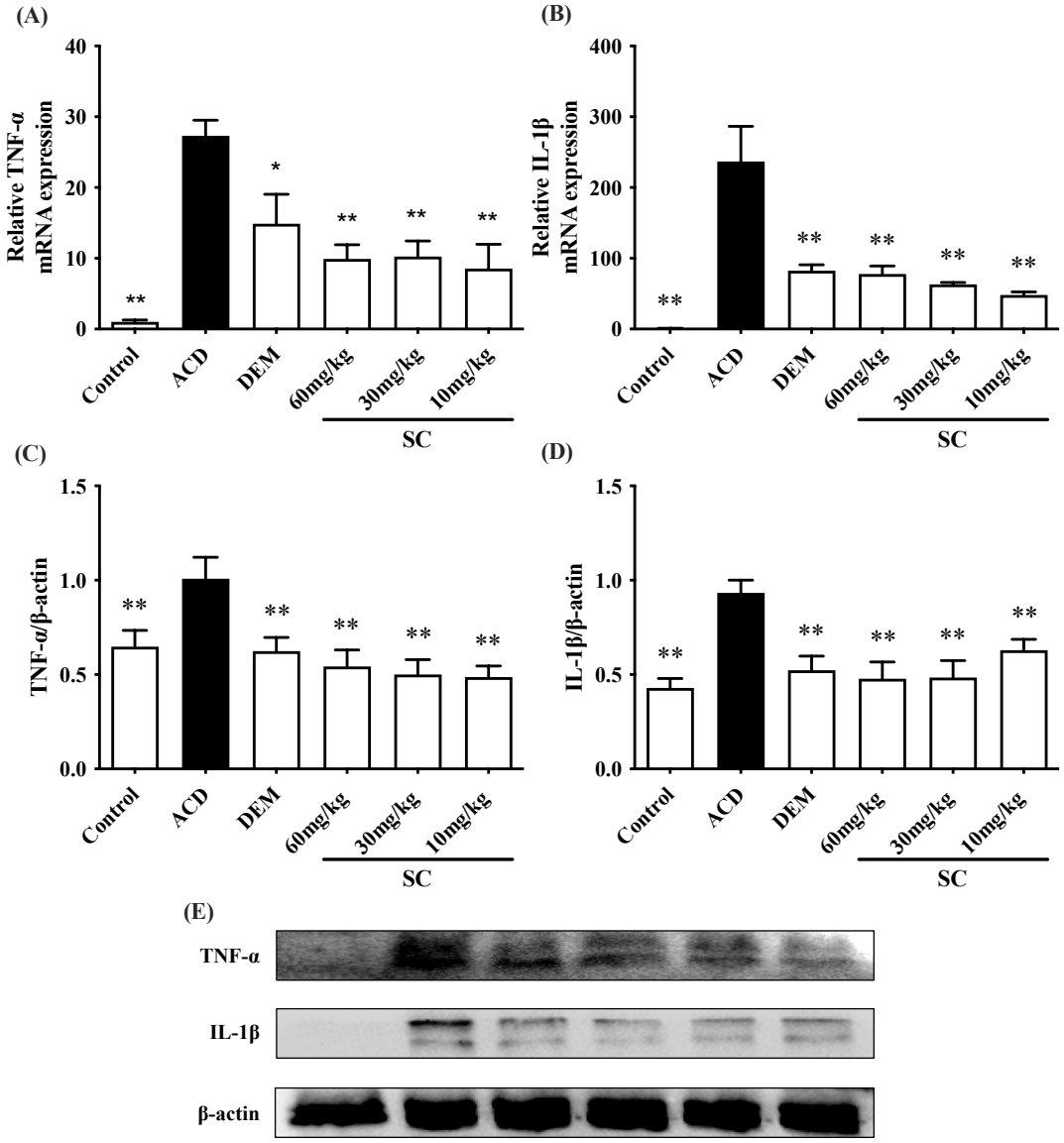

Figure 4. Effects of SC on proinflammatory factors in the skin on ACD mouse model. The mRNA expression of TNF-α (A) and IL-1β (B) were obtained from cheek skin for different groups of mice. The mRNA data are presented as $2^{-\Delta\Delta Ct}$ values relative to β-actin. Protein expression of TNF-α (C) and IL-1β (D) and representative of western blots (E) respectively. $^{*}p < 0.05$, $^{**}p < 0.01$ for significance compared with the ACD group, error bars: S.E.M. n = 3-5 mice/group.

3.5 SC downregulated the expression of the TRPA1 & TRPV1 in TG

Expression of TRPA1 and TRPV1 mRNA in TG was significantly greater in the

ACD group, compared with that of the control group (Figure 5A, 5B). Compared with the ACD group, CPZ and SC significantly downregulated TRPV1 and TRPA1 mRNA expression. (Figure 5A, 5B). At the protein level, significantly higher TRPA1 and TRPV1 protein expression was identified in the ACD group compared with the control group (Figure 5C, 5D). Compared with the ACD group, CPZ had no effect, whereas SC decreased TRPA1 and TRPV1 protein expression (Figure 5C, 5D).

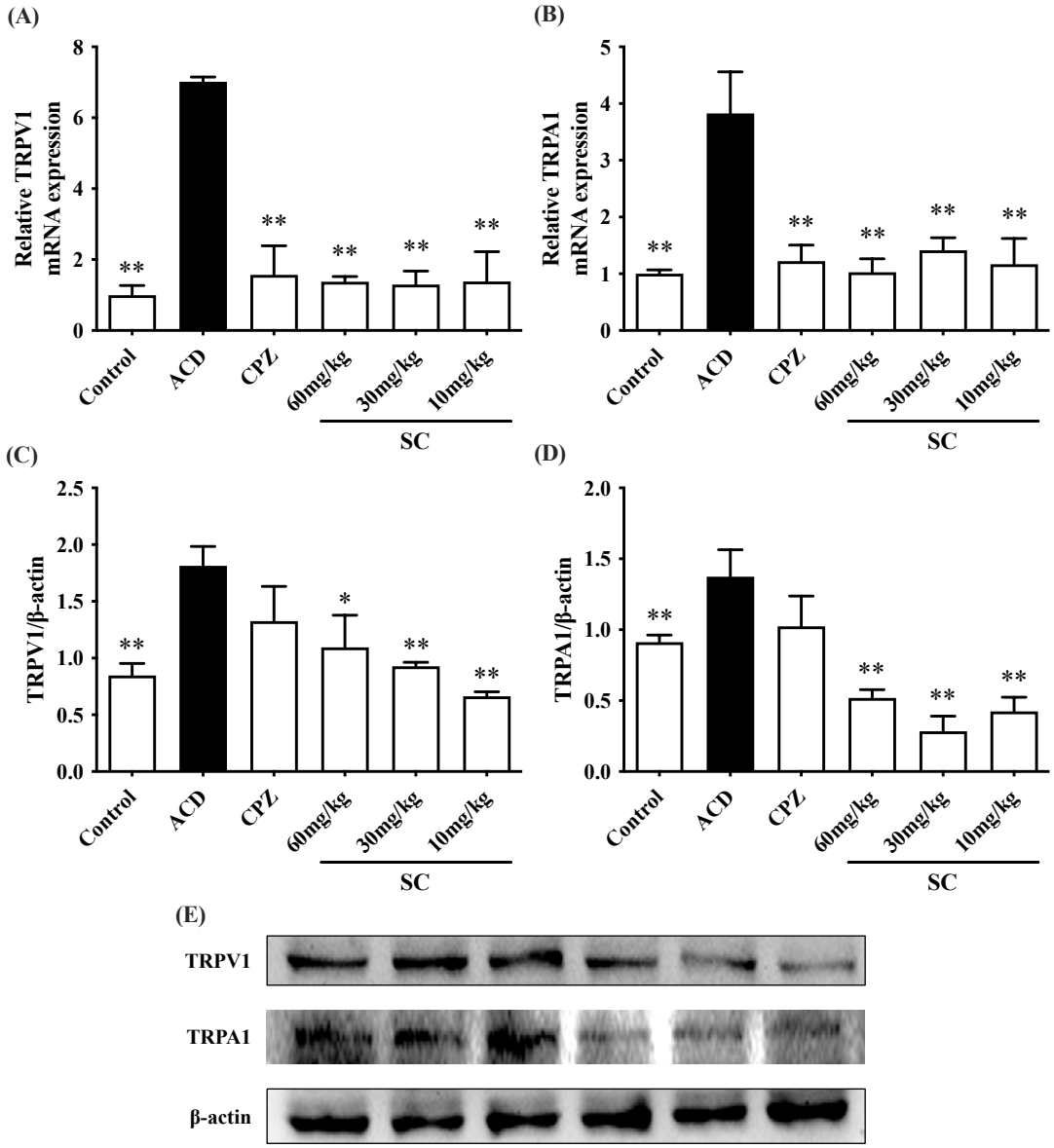

Figure 5. Effects of SC on TRP channels expression in TG of ACD mouse model. The mRNA expression levels of TRPV1 (A) and TRPA1 (B) were obtained from TG for

283 different groups of mice. The mRNA data are presented as $2^{-\Delta\Delta Ct}$ values relative to
284 β-actin. The protein expression of TRPV1 (C) and TRPA1 (D), and exemplary images
285 of western blotting (E). $^{*}p < 0.05$, $^{**}p < 0.01$ for significance compared with the ACD
286 group, error bars: S.E.M. n = 3-5 mice/group.

287 **3.6 SC reduced scratching and wiping behavior induced by AITC and CAP**

288 To determine whether SC targets TRPA1 and/or TRPV1, 10 mg/kg SC was
289 administrated i.g. before treatment with AITC or CAP. The numbers of scratching
290 bouts and wipes were significantly increased after the AITC administration (Figure
291 6A, 6B), while only wipes were significantly increased after CAP administration
292 (Figure 6E, 6F). The wipes peaked at 5 min after ATIC and CAP administration, while
293 the scratching bouts peaked at 25 min after ATIC administration (Figure 6D, 6H, 6C).
294 The scratching bout was not significantly induced by CAP (Figure 6G). SC
295 significantly decreased scratching bouts induced by AITC and wipes induced by
296 AITC and CAP (Figure 6A, 6B, 6F).

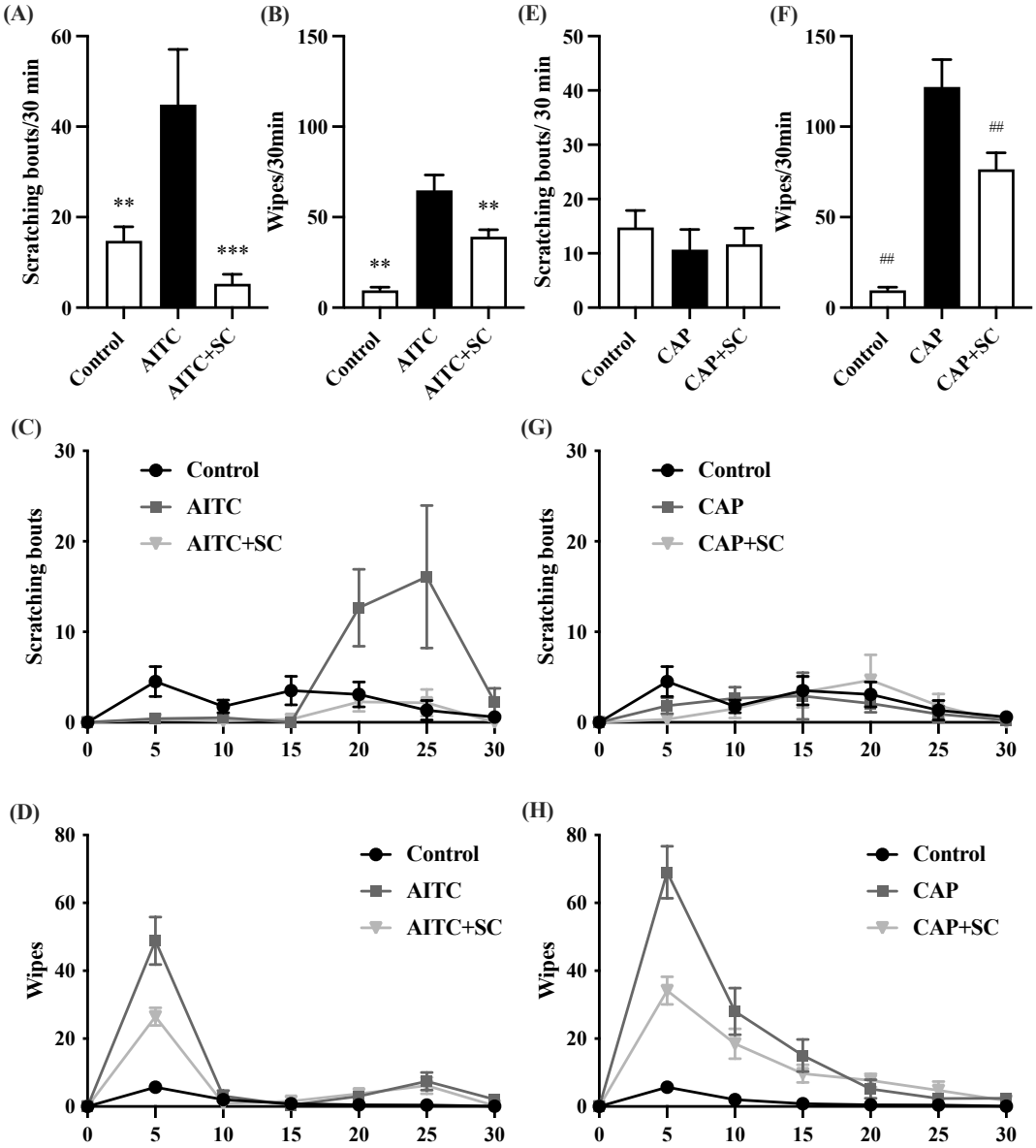

Figure 6. Effect of SC in AITC-induced and CAP-induced wiping and scratching behavior. The numbers of scratching bouts (A) and wipes (B) were evaluated for 30 min after AITC injection at 1 h after SC administration. The numbers of scratching bouts (E) and wipes (F) were evaluated for 30 min after CAP injection at 1 h after SC administration. The time course of scratching bouts (C) and wipes (D) after AITC injection at 1 h after administration. The time course of scratching bouts (G) and wipes (H) after AITC injection at 1 h after administration. $^{*}p < 0.05$, $^{**}p < 0.01$ for

305 significance compared with AITC group, $^{\#}p < 0.05$, $^{\#\#}p < 0.01$ for significance
306 compared with CAP group, error bars: S.E.M, n=10 mice/group.

307 **3.7 SC as a competitive inhibitor of TRPA1 and TRPV1**

308 To further investigate the relationship between SC, AITC, CAP and TRPV1,
309 TRPA1, molecular docking simulation was performed *in silico* by Autodock Vina and
310 Chimera/ChimeraX, with small molecules, or ligands, of SC, AITC and CAP, and
311 target protein, or receptors, of TRPV1 and TRPA1 tetramers. The highest binding
312 energies estimated between SC and TRPV1 or TRPA1 were higher than that of AITC,
313 but lower than that of CAP. All ligands can form hydrogen bonds with receptors
314 except for AITC and TRPV1 (Table 2, Figure 7). The atom distance between ligands
315 and receptors estimated between SC and TRPV1 or TRPA1 was lower than that of
316 AITC but higher than that of CAP.

317 Table 2 Estimated binding energy by molecular docking

Ligand	**Receptor**	**KCal/mol**	**Binding Type**	**Binding Site**	**Atoms Distance(Å)**
SC	TRPA1	-6.1	Hydrogen	Ser364	2.186
	TRPV1	-6.4	Hydrogen	Glu1367	2.195
AITC	TRPA1	-3.5	Hydrogen	Ser864	2.355
	TRPV1	-3.4	Van der Waals		
CAP	TRPA1	-6.9	Hydrogen	Lys708	1.996
	TRPV1	-7.1	Hydrogen	Tyr1320	2.122

318

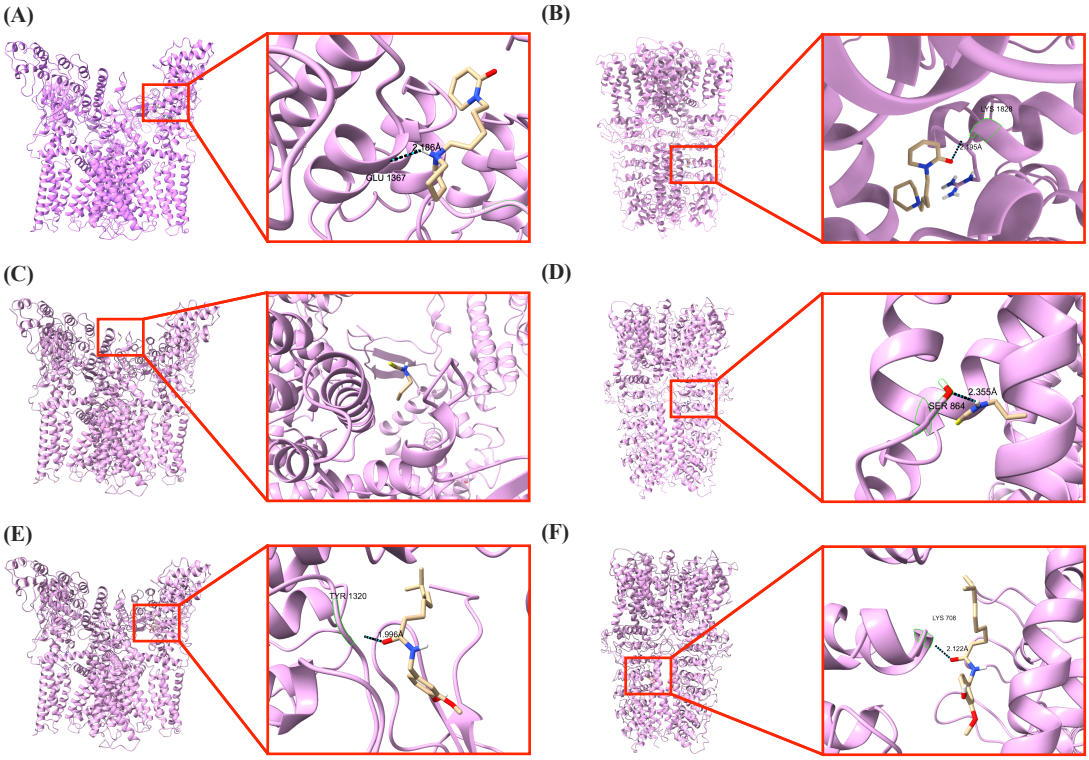

Figure 7. Estimated optimal binding conformations by docking simulation of ligands (small molecules, in yellow) to receptors (proteins, in purple). SC was docked onto (A) TRPV1 and (B) TRPA1; AITC was docked onto (C) TRPV1 and (D) TRPA1; CAP was docked onto (E) TRPV1 and (F) TRPA1. The distance of the hydrogen bonds between ligands and receptors was calculated.

To further investigate the relationship between SC, AITC, and CAP when binding to TRPV1 and TRPA1, the competition of docking results was visualized by ChimeraX. SC may compete with AITC by binding to TRPV1 monomer at SER284, GLU287 in the Linker domain, LEU438, ARG 442 in the S4-S5 linker, and GLN562 in the TRP domain (Figure 8A), and by binding to TRPA1 monomer at sites of ASN145, LYS146, ARG147, LYS148 in AR16 and LYS528 in the C-terminal coiled-coil (Figure 8C), or disturbing AITC binding to ILE234, GLU235, ARG238 in the Pre-S1 helix and LEU479, SER521 in the TRP-like domain by Van der Waals. SC

333 may compete with CAP by binding to TRPV1 monomer at GLU287, ARG299 in the
334 Linker domain, SER397 in the S3, ARG442 in the S4-S5 linker, and LYS576 in the
335 TRP domain (Figure 8B).

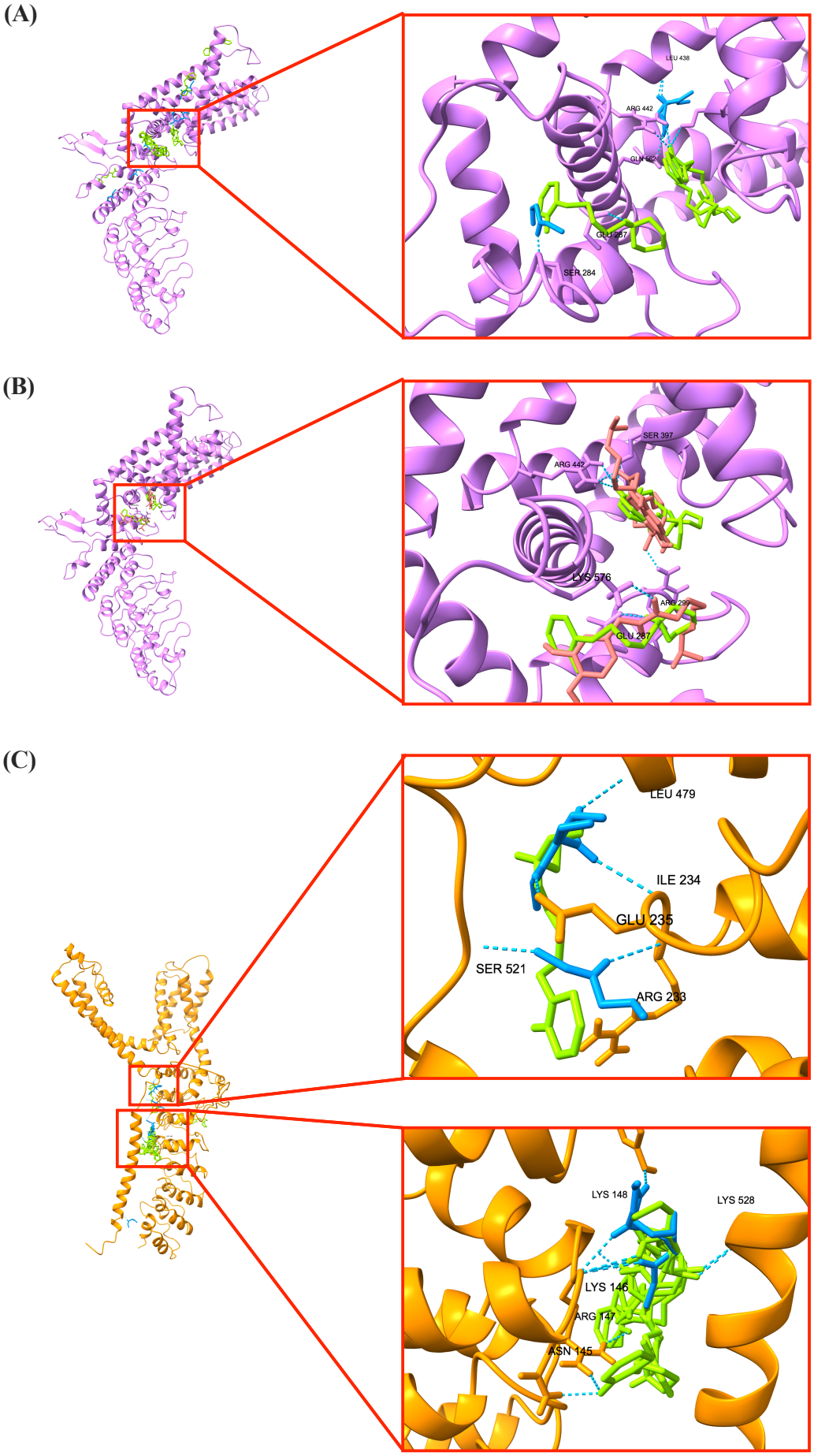
(A)
LEU 438
ARG 442
GLU 287
SER 284
(B)
SER 397
ARG 442
LYS 576
ARG 299
GLU 287
(C)
LEU 479
ILE 234
GLU 235
SER 521
ARG 233
LYS 148
LYS 528
LYS 146
ARG 147
ASN 145

337 Figure 8. The potential competition between SC and AITC/CAP on TRPV1 and
338 TRPA1 monomers. (A) SC (green) and AITC (blue), and (B) SC and CAP (red)
339 competed in one protein pocket of TRPV1 (purple); (C) SC (green) and AITC (blue)
340 competed on different binding sites in two protein pockets of TRPA1 (orange).
341

342 # 4. Discussion

343 Spontaneous itch and pain are of paramount clinical relevance being the main
344 complaint of chronic itch and pain patients (3). SC was screened from SFR by our
345 research group which showed a binding ability to DRG cells (11). In the present study,
346 the anti-pruritic and analgesic effects of SC were tested in a SADBE-induced ACD
347 mouse model manifesting both itch and pain. Our results revealed that SC possesses
348 strong anti-pruritic and analgesic effects. Expression of mRNA and protein of TRPA1
349 and TRPV1 in SC treatment groups was decreased compared to the ACD group.
350 Furthermore, *in vivo* experiments showed that SC reduces AITC-induced wiping and
351 scratching behavior and CAP-induced wiping behavior thus indicating that SC
352 inhibits both TRPV1 and TRPA1. Molecular docking revealed the potential of SC as a
353 competitive inhibitor of both TRPV1 and TRPA1, compared with AITC and CAP.
354 Therefore, we posit that SC can relieve itch and pain in ACD by downregulating
355 expression and inhibiting the function of TRPV1 and TRPA1.

356 The patterns of peripheral and central sensitization linked to chronic itch and
357 pain are remarkably similar (3). In the clinic, ACD-associated itch symptoms are often
358 presented with repeated long-lasting episodes and are sometimes accompanied by

359 pain sensation (20). SADBE is most commonly used for the treatment of pelade and
360 warts but often causes ACD with severe itch after frequent applications, and hence
361 SADBE is commonly used in ACD studies (21). Consistent with clinical observations,
362 SADBE effectively induces ACD in mice, which display significant spontaneous
363 scratching and wiping behavior (22). In the present study, SADBE was used to induce
364 the ACD mouse model; SABDE increased scratching bouts and wipes significantly as
365 has been described previously (23).

366 SFR is widely used in relieving inflammatory itch and pain. Oxymatrine,
367 screened from SFR together with SC by our research group, has already been tested
368 and demonstrated anti-pruritic and anti-inflammatory effects in ACD mice (11, 12). It
369 was previously shown that SC possessed significant anti-nociceptive activity in
370 thermally and chemically induced mouse pain models, and anti-inflammatory activity
371 on carrageenan-induced rat hind paw edema, xylene-induced mouse ear edema and
372 acetic acid-induced mouse vascular permeation (24). In the present study, the
373 anti-pruritic effect of SC was additionally evaluated and all these three effects were
374 tested on the same mouse model, with 10 mice for each group to reduce the individual
375 difference. Our results revealed that SC significantly reduces scratching bouts and
376 wipes in the ACD mice, thus showing a strong anti-pruritic and analgesic effect. The
377 PASI score and skin fold thickness measurement showed that SC also relieved the
378 SADBE-induced inflammation reaction. TNF-α is the major cytokine involved in
379 chronic inflammation inducing IL-1β and other interleukins for inflammatory
380 signaling cascades. In the present study, SC downregulated mRNA and protein

381 expression of TNF-α and IL-1β as good as dexamethasone in the ACD model.

382 TRPA1 and TRPV1 are both involved in inflammatory pain and were suggested
383 to mediate histamine-independent and histamine-dependent itch, respectively (7).
384 Both TRPA1 and TRPV1 are required for generating spontaneous scratching in the
385 SADBE-induced ACD mouse model by directly promoting the excitability of
386 pruriceptors (25). In the present study, we found that TRPA1 and TRPV1 in TG were
387 upregulated and increased after the SADBE application, consistent with previous data
388 from the dorsal root ganglia.

389 $TRPA1^{-/-}$ mice manifest fewer pain responses when injected with bradykinin or
390 ATIC (26). Mice lacking TRPA1 display reduced scratching and skin lesion severity,
391 highlighting a role for TRPA1 in acute and chronic itch, and suggesting that TRPA1
392 antagonists may be useful for treating various pathological itch conditions (27).
393 Nevertheless, mice lacking TRPA1 and subjected to histamine-independent itch
394 modeling showed less reduction of scratching response to cutaneous application of
395 borneol (28). Expression of TRPA1 was upregulated in patients who suffer from
396 severe itch (29). The mRNA of TRPA1 was upregulated in neuropathic pain whereas
397 the protein of TRPA1 was increased in inflammatory pain in dorsal root ganglia (30,
398 31). TRPA1 also contributed to pruritus in allergic contact dermatitis (32, 33). Our
399 results demonstrated that SC downregulates the TRPA1 expression and reduces the
400 scratching and wiping behaviors induced by ATIC, similar to HC-030031 (34).
401 Molecular docking showed lower binding energy and a smaller atomic distance of
402 hydrogen bond between SC and TRPA1, indicating that SC could be a potential

403 competitive inhibitor of TRPA1, compared with AITC. Thus, we suggest that SC
404 efficiently inhibits the function and downregulates the expression of TRPA1 to relieve
405 itch and pain in diseases such as ACD.

406 TRPV1 is expressed at the highest level in peripheral sensory neurons involved
407 in the perception of pain (35). The first evidence of the role of TRPV1 in peripheral
408 pain processing arose from observations made in mice injected with the TRPV1
409 antagonist CPZ (36, 37). TRPV1 contributes to both acute and chronic itch conditions
410 (38). CPZ pretreatment reduced the scratching bouts induced by the subcutaneous
411 injection of histamine into mice's necks (39). The anti-pruritic and analgesic effect of
412 CPZ was also observed in our present study in the SADBE-induced ACD mouse
413 model. A point mutation in the coding of the S4-S5 linker in the *Trpv1* gene reduced
414 TRPV1 phosphorylation and cell membrane recruitment, successively reducing pain
415 and histamine-dependent itch (40). Oleic acid, a natural compound, also inhibits
416 TRPV1 thus modulating itch and pain (41). We also showed that SC downregulated
417 the mRNA and protein expression of TRPV1. Our behavioral tests showed that
418 CAP-induced wiping was reduced by pretreatment of SC, hinting that SC could
419 inhibit TRPV1. Molecular docking showed competitive binding energy and atomic
420 distance of hydrogen bond between SC and TRPV1, indicating that SC may be a
421 potential competitive inhibitor of TRPV1 Thus, we suggest that SC could efficiently
422 inhibit and downregulate the expression of TRPV1 to relieve itch and pain manifested
423 in diseases such as ACD.

424 Molecular docking simulations demonstrated that SC is competing on the

425 intracellular AR16, the C-terminal coiled-coil, the membrane Pre-S1 helix and the
426 TRP-like domain in the TRPA1 monomer with AITC, and competing on the Linker
427 domain, the S4-S5 linker, and the TRP domain in the TRPV1 monomer with AITC
428 and CAP. Although the amino acid numbers differ, the binding pocket around the
429 S4-S5 linker in TRPV1 of SC competing with AITC or CAP simulated in this study is
430 quite similar to the previously published simulation of CAP binding to TRPV1,
431 referring to the TRPV1 structure identified (42, 43). While the major simulations of
432 AITC and SC demonstrated lower binding energy to the intracellular AR16 or the
433 Linker domain in the N-terminus, the disturbance of SC in the Pre-S1 helix and the
434 TRP-like domain seems more convincing, compared to the simulation of DNCB and
435 DNFB, agonists of TRPA1 to trigger itch as AITC, binding to TRPA1 in protein
436 pockets around the Linker domain and the TRP-like domain (44). Further studies
437 focusing on protein pockets identified to testify whether SC is a competitive inhibitor
438 of TRPV1 and TRPA1 are needed.

439 In conclusion, SC demonstrated a strong anti-inflammatory, anti-pruritic and
440 analgesic effect by targeting TRP channels in TG. These findings suggest that SC
441 might have significant therapeutic potential in treating inflammatory itch and pain.

442 5. Conflict of interest

443 The authors declare no conflicts of interest.

444 6. Author contributions

445 H.Z. and Z.Z. collected and analyzed the data. H.Z., P. L. collected the samples. The

mice cheeks were scored by D.Z. and Z.Z. The video analysis was done with assistance from P.L. and D.Z. H.N. and A.V. designed the experiments. The paper was written by H.Z., and modified by H.N and A.V. The research is supervised by H.N.

7. Acknowledgements

This work was supported by grants from the Chinese National Natural Science Foundation to H.N. (No. 81373993 & No. 81861138042).

8. References

1. Dhand A, Aminoff MJ. The neurology of itch. Brain. 2014;137(Pt 2):313-22.
2. Miyamoto T, Patapoutian A. Why Does Morphine Make You Itch? Cell. 2011;147(2):261-2.
3. Li C, Kim HJ, Back SK, Na HS. Common and discrete mechanisms underlying chronic pain and itch: peripheral and central sensitization. Pflugers Arch. 2021;473(10):1603-15.
4. Yamaguchi J, Aihara M, Kobayashi Y, Kambara T, Ikezawa Z. Quantitative analysis of nerve growth factor (NGF) in the atopic dermatitis and psoriasis horny layer and effect of treatment on NGF in atopic dermatitis. J Dermatol Sci. 2009;53(1):48-54.
5. Nilius B, Owsianik G. The transient receptor potential family of ion channels. Genome Biology. 2011;12(3):218.
6. Tsagareli MG, Nozadze I. An overview on transient receptor potential channels superfamily. Behav Pharmacol. 2020;31(5):413-34.
7. Moore C, Gupta R, Jordt SE, Chen Y, Liedtke WB. Regulation of Pain and Itch by TRP Channels. Neurosci Bull. 2018;34(1):120-42.
8. Basbaum AI, Bautista DM, Scherrer G, Julius D. Cellular and molecular mechanisms of pain. Cell. 2009;139(2):267-84.

9. Shim WS, Tak MH, Lee MH, Kim M, Kim M, Koo JY, et al. TRPV1 mediates histamine-induced itching via the activation of phospholipase A2 and 12-lipoxygenase. J Neurosci. 2007;27(9):2331-7.

10. Wilson SR, Gerhold KA, Bifolck-Fisher A, Liu Q, Patel KN, Dong X, et al. TRPA1 is required for histamine-independent, Mas-related G protein-coupled receptor-mediated itch. Nat Neurosci. 2011;14(5):595-602.

11. Zhang Z, Pan J, Zhu T, Malewicz N, Ye K, Rong J, et al. Oxymatrine screened from Sophora flavescens by cell membrane immobilized chromatography relieves histamine-independent itch. J Pharm Pharmacol. 2021;73(12):1617-29.

12. Xu X, Xiao W, Zhang Z, Pan J, Yan Y, Zhu T, et al. Anti-pruritic and anti-inflammatory effects of oxymatrine in a mouse model of allergic contact dermatitis. J Dermatol Sci. 2018.

13. Shimada SG, LaMotte RH. Behavioral differentiation between itch and pain in mouse. Pain. 2008;139(3):681-7.

14. Friedman RM, Khalsa PS, Greenquist KW, LaMotte RH. Neural coding of the location and direction of a moving object by a spatially distributed population of mechanoreceptors. J Neurosci. 2002;22(21):9556-66.

15. Irwin JJ, Tang KG, Young J, Dandarchuluun C, Wong BR, Khurelbaatar M, et al. ZINC20-A Free Ultralarge-Scale Chemical Database for Ligand Discovery. J Chem Inf Model. 2020;60(12):6065-73.

16. Burley SK, Bhikadiya C, Bi C, Bittrich S, Chao H, Chen L, et al. RCSB Protein Data Bank (RCSB.org): delivery of experimentally-determined PDB structures alongside one million computed structure models of proteins from artificial intelligence/machine learning. Nucleic Acids Res. 2023;51(D1):D488-d508.

17. Trott O, Olson AJ. AutoDock Vina: improving the speed and accuracy of docking with a new scoring function, efficient optimization, and multithreading. J Comput Chem. 2010;31(2):455-61.

18. Pettersen EF, Goddard TD, Huang CC, Couch GS, Greenblatt DM, Meng EC, et al. UCSF Chimera--a visualization system for exploratory research and analysis. J Comput Chem. 2004;25(13):1605-12.

19. Pettersen EF, Goddard TD, Huang CC, Meng EC, Couch GS, Croll TI, et al. UCSF ChimeraX: Structure visualization for researchers, educators, and developers. Protein Sci. 2021;30(1):70-82.

20. LaMotte RH. Allergic Contact Dermatitis: A Model of Inflammatory Itch and Pain in Human and Mouse. Adv Exp Med Biol. 2016;904:23-32.

21. Mastrolonardo M, Lopalco PL, Diaferio A. Topical immunotherapy with contact sensitizers: a model to study the natural history of delayed hypersensitivity. Contact Dermatitis. 2002;47(4):210-4.

22. Qu L, Fan N, Ma C, Wang T, Han L, Fu K, et al. Enhanced excitability of MRGPRA3- and MRGPRD-positive nociceptors in a model of inflammatory itch and pain. Brain. 2014;137(Pt 4):1039-50.

23. Zhang Z, Malewicz NM, Xu X, Pan J, Kumowski N, Zhu T, et al. Differences in itch and pain behaviors accompanying the irritant and allergic contact dermatitis produced by a contact allergen in mice. Pain Rep. 2019;4(5):e781.

24. Gao Y, Li G, Li C, Zhu X, Li M, Fu C, et al. Anti-nociceptive and anti-inflammatory activity of sophocarpine. J Ethnopharmacol. 2009;125(2):324-9.

25. Feng J, Yang P, Mack MR, Dryn D, Luo J, Gong X, et al. Sensory TRP channels contribute differentially to skin inflammation and persistent itch. Nat Commun. 2017;8(1):980.

26. Bautista DM, Jordt SE, Nikai T, Tsuruda PR, Read AJ, Poblete J, et al. TRPA1 mediates the inflammatory actions of environmental irritants and proalgesic agents. Cell. 2006;124(6):1269-82.

27. Morita T, McClain SP, Batia LM, Pellegrino M, Wilson SR, Kienzler MA, et al. HTR7 Mediates Serotonergic Acute and Chronic Itch. Neuron. 2015;87(1):124-38.

28. Tian W, He D, Liu J, Chen F, Zhang W, Hu J, et al. Topical borneol relieves nonhistaminergic pruritus via targeting TRPA1 and TRPM8 channels in peripheral nerve terminals of mice. Eur J Pharmacol. 2023;953:175833.

29. Yang YS, Cho SI, Choi MG, Choi YH, Kwak IS, Park CW, et al. Increased expression of three types of transient receptor potential channels (TRPA1, TRPV4 and TRPV3) in burn scars with post-burn pruritus. Acta Derm Venereol. 2015;95(1):20-4.

30. Caspani O, Zurborg S, Labuz D, Heppenstall PA. The contribution of TRPM8 and TRPA1 channels to cold allodynia and neuropathic pain. PLoS One. 2009;4(10):e7383.

31. Martínez-Rojas VA, Salinas-Abarca AB, Gómez-Víquez NL, Granados-Soto V, Mercado F, Murbartián J. Interaction of NHE1 and TRPA1 Activity in DRG Neurons Isolated from Adult Rats and its Role in Inflammatory Nociception. Neuroscience. 2021;465:154-65.

32. Liu B, Tai Y, Achanta S, Kaelberer MM, Caceres AI, Shao X, et al. IL-33/ST2 signaling excites sensory neurons and mediates itch response in a mouse model of poison ivy contact allergy. Proc Natl Acad Sci U S A. 2016;113(47):E7572-e9.

33. Liu B, Escalera J, Balakrishna S, Fan L, Caceres AI, Robinson E, et al. TRPA1 controls inflammation and pruritogen responses in allergic contact dermatitis. Faseb j. 2013;27(9):3549-63.

34. Fischer L, Lavoranti MI, de Oliveira Borges M, Miksza AF, Sardi NF, Martynhak BJ, et al. TRPA1, substance P, histamine and 5-hydroxytryptamine interact in an interdependent way to induce nociception. Inflamm Res. 2017;66(4):311-22.

35. Caterina MJ, Julius D. The vanilloid receptor: a molecular gateway to the pain pathway. Annu Rev Neurosci. 2001;24:487-517.

36. Caterina MJ, Leffler A, Malmberg AB, Martin WJ, Trafton J, Petersen-Zeitz KR, et al. Impaired nociception and pain sensation in mice lacking the capsaicin receptor. Science. 2000;288(5464):306-13.

37. Davis JB, Gray J, Gunthorpe MJ, Hatcher JP, Davey PT, Overend P, et al. Vanilloid receptor-1 is essential for inflammatory thermal hyperalgesia. Nature. 2000;405(6783):183-7.

38. Sun S, Dong X. Trp channels and itch. Semin Immunopathol. 2016;38(3):293-307.

39. Hondoh A, Ishida Y, Ugawa S, Ueda T, Shibata Y, Yamada T, et al. Distinct expression of cold receptors (TRPM8 and TRPA1) in the rat nodose-petrosal ganglion complex. Brain Res. 2010;1319:60-9.

40. Duo L, Hu L, Tian N, Cheng G, Wang H, Lin Z, et al. TRPV1 gain-of-function

561 mutation impairs pain and itch sensations in mice. Mol Pain.
562 2018;14:1744806918762031.
563 41. Morales-Lázaro SL, Llorente I, Sierra-Ramírez F, López-Romero AE,
564 Ortíz-Rentería M, Serrano-Flores B, et al. Inhibition of TRPV1 channels by a
565 naturally occurring omega-9 fatty acid reduces pain and itch. Nat Commun.
566 2016;7:13092.
567 42. Domene C, Darré L, Oakes V, Gonzalez-Resines S. A Potential Route of
568 Capsaicin to Its Binding Site in the TRPV1 Ion Channel. J Chem Inf Model.
569 2022;62(10):2481-9.
570 43. Liao M, Cao E, Julius D, Cheng Y. Structure of the TRPV1 ion channel
571 determined by electron cryo-microscopy. Nature. 2013;504(7478):107-12.
572 44. Wu H, Niu C, Qu Y, Sun X, Wang K. Selective activation of TRPA1 ion channels
573 by nitrobenzene skin sensitizers DNFB and DNCB. J Biol Chem.
574 2022;298(2):101555.
575